

An empirical expression for ϵ_θ on the axis of a slightly heated turbulent round jet

J. Lemay^{1,†}, L. Djenidi², R. A. Antonia² and A. Benaïssa³

¹Department of Mechanical Engineering, Université Laval, 1065 avenue de la Médecine, Québec City, QC G1V 0A6, Canada

²Discipline of Mechanical Engineering, School of Engineering, University of Newcastle, Newcastle, 2308 NSW, Australia

³Department of Mechanical and Aerospace Engineering, Royal Military College of Canada, PO Box 17000, Station Forces, Kingston, ON K7K 7B4, Canada

(Received 20 June 2018; revised 22 January 2019; accepted 18 February 2019;
first published online 22 March 2019)

Self-preservation analyses of the equations for the mean temperature and the second-order temperature structure function on the axis of a slightly heated turbulent round jet are exploited in an attempt to develop an analytical expression for ϵ_θ , the mean dissipation rate of $\bar{\theta}^2/2$, where $\bar{\theta}^2$ is the temperature variance. The analytical approach follows that of Thiesset *et al.* (*J. Fluid Mech.*, vol. 748, 2014, R2) who developed an expression for ϵ_k , the mean turbulent kinetic energy dissipation rate, using the transport equation for $\overline{(\delta u)^2}$, the second-order velocity structure function. Experimental data show that complete self-preservation for all scales of motion is very well satisfied along the jet axis for streamwise distances larger than approximately 30 times the nozzle diameter. This validation of the analytical results is of particular interest as it provides justification and confidence in the analytical derivation of power laws representing the streamwise evolution of different physical quantities along the axis, such as: η , λ , λ_θ , R_U , R_θ (all representing characteristic length scales), the mean temperature excess Θ_0 , the mixed velocity–temperature moments $\overline{u\theta^2}$, $\overline{v\theta^2}$ and $\overline{\theta^2}$ and ϵ_θ . Simple models are proposed for $\overline{u\theta^2}$ and $\overline{v\theta^2}$ in order to derive an analytical expression for A_{ϵ_θ} , the prefactor of the power law describing the streamwise evolution of ϵ_θ . Further, expressions are also derived for the turbulent Péclet number and the thermal-to-mechanical time scale ratio. These expressions involve global parameters that are most likely to be influenced by the initial and/or boundary conditions and are therefore expected to be flow dependent.

Key words: jets, turbulence modelling

1. Introduction

Turbulent jets involving a scalar continue to interest researchers for both fundamental reasons and because of many industrial applications. The latter can range from the dispersal of pollution to the design of devices optimizing the mixing of a scalar

† Email address for correspondence: jean.lemay@gmc.ulaval.ca

quantity. An important characteristic of the round jet is that all scales of motion can satisfy the requirements of self-preservation. Particularly along its axis, turbulence decays according to well-defined power laws. As a consequence, the turbulent and local Reynolds numbers (Djenidi *et al.* 2016, hereafter referred to as DALL), defined as $Re_\lambda \equiv \sqrt{\overline{u^2}}\lambda/\nu$ and $Re_0 \equiv U_0 R_U/\nu$, respectively are constant. Here, the overbar denotes time-averaged quantities defining one-point statistics, ν is the kinematic viscosity, $\lambda \equiv (\overline{u^2}/(\partial u/\partial x)^2)^{1/2}$ is the Taylor microscale. In what follows, ϵ_k is the mean dissipation rate of k , the turbulent kinetic energy, $k \equiv (\overline{u^2} + \overline{v^2} + \overline{w^2})/2$; u , v and w are respectively the fluctuating velocity components in the streamwise (x), radial (r) and azimuthal (φ) directions, U_0 is the mean streamwise velocity on the jet axis and R_U is the jet half-radius. The constancy of Re_λ with x implies that self-preservation should apply irrespective of the scaling parameters used, provided they comply with self-preservation. The combinations ($\eta \equiv (\nu^3/\epsilon_k)^{1/4}$ and $\nu_K \equiv (\nu\epsilon_k)^{1/4}$) or (λ and $\sqrt{\overline{u^2}}$), (R_U and U_0) can therefore be employed interchangeably (see DALL).

It is well established from free shear flow similarity analysis (see for example Tennekes & Lumley 1972; Pope 2000) that a turbulent round jet spreads linearly, *viz.* $R_U \propto x$, and that $U_0 \propto x^{-1}$ and $\overline{u^2} \propto x^{-2}$. These results are traditionally derived from the mean flow equations written by assuming the thin shear-layer approximation. More recently, starting with the transport equation for $(\delta u)^2$ or, equivalently, a scale-by-scale (sbs) kinetic energy budget equation (Burattini, Antonia & Danaila 2005a), Thiesset, Antonia & Djenidi (2014) (hereafter referred to as TAD) carried out a two-point self-preservation analysis on the axis of a turbulent round jet. They showed that ϵ_k evolves longitudinally as a -4 th power law, *viz.*

$$\frac{\epsilon_k D}{U_j^3} = A_{\epsilon_k} \hat{x}^{-4}, \tag{1.1}$$

where $\hat{x} = (x - x_0)/D$ (x_0 is a virtual origin, D is the nozzle diameter, U_j is the jet exit velocity), and A_{ϵ_k} is a constant to be determined. The assumptions made by these authors (isotropy of dissipative scales and negligible contributions from turbulent and pressure diffusion terms in the k budget) differ from the usual assumption ($C_\epsilon = \epsilon_k L_u/u^3 = \text{const.}$) which underpins the well-known -4 th power law for ϵ_k in the far field of a round jet (see for example Friehe, Van Atta & Gibson 1971; Antonia, Satyaprakash & Hussain 1980; Mi, Xu & Zhou 2013). Further, DALL derived the following power laws, $U_0 \propto \hat{x}^{-1}$, $k \propto \hat{x}^{-2}$, $\epsilon_k \propto \hat{x}^{-4}$ and $l_q \propto \hat{x}$ (where l_q is the characteristic length scale) from their analysis based on the application of self-preservation to the sbs energy budget. The main difference, relative to previous studies, relies on the fact that the conservation of (simplified) mean momentum and mean turbulent kinetic energy equations were not required. Of particular relevance to the present study, TAD obtained an expression for the prefactor of the -4 th power law for ϵ_k defined by (1.1):

$$A_{\epsilon_k} = B_U^3 A_I^2 (2 + \mathcal{R}), \tag{1.2}$$

where $A_I = \sqrt{\overline{u^2}}/U_0$ and $\mathcal{R} = \overline{v^2}/\overline{u^2}$, two constant parameters along the jet axis (as required by self-preservation), and B_U is the coefficient in $U_0/U_j = B_U \hat{x}^{-1}$. Considering R_U and U_0 to be the relevant outer local scales for the k budget, the normalized form of the mean dissipation rate can be written as

$$\epsilon_k^* = \frac{\epsilon_k R_U}{U_0^3} = B_{R_U} A_I^2 (2 + \mathcal{R}). \tag{1.3}$$

Hereafter, * stands for normalization with R_U and U_0 . Based on DALL's analysis, self-preservation on the jet axis requires that $\epsilon_k^* = \text{const}$.

Otherwise, from measurements of the one-point turbulent kinetic energy budget, Panchapakesan & Lumley (1993a) and Darisse, Lemay & Benaïssa (2015) observed on the jet axis that the mean dissipation rate is essentially compensated by convection (C_k^*) and production (P_k^*), viz. $\epsilon_k^* \simeq C_k^* + P_k^*$. Using self-preservation forms for k , \bar{U} and \bar{V} , Darisse *et al.* (2015) derived the explicit relations for C_k^* and P_k^* on the jet axis. Using axisymmetry, the continuity equation, the power-law expressions for U_0 and R_U and the notation introduced by TAD, viz. A_I and \mathcal{R} , with $k/U_0^2 = A_I^2(\mathcal{R} + 1/2)$, the normalized convection and production terms can finally be written as

$$C_k^* = 2B_{R_U}A_I^2(\mathcal{R} + 1/2), \quad (1.4)$$

$$P_k^* = B_{R_U}A_I^2(\mathcal{R} - 1). \quad (1.5)$$

The sum of these equations gives

$$\epsilon_k^* \simeq C_k^* + P_k^* = B_{R_U}A_I^2(\mathcal{R} + 2). \quad (1.6)$$

This indicates that relation (1.3) represents essentially the sum of the convection and production terms of the normalized form of the k budget written on the jet axis. Darisse *et al.* (2015) showed that this relation was in very good agreement with ϵ_k inferred as the remainder of their k budget.

In this paper we extend the analysis of DALL and TAD to a slightly heated turbulent round jet with a view to developing an analytical expression for ϵ_θ on the jet axis. The analysis is restricted to small values of Θ_j , the mean temperature excess relative to ambient at the jet exit, in order to allow temperature to be treated as a passive scalar. The power law $\epsilon_\theta \propto \hat{x}^{-4}$, describing the evolution of ϵ_θ along the jet axis, is derived in §2 by applying self-preservation to the sbs budget of $\bar{\theta}^2/2$. This rigorous derivation is new and particularly relevant, because it does not involve any of the *ad hoc* assumptions usually made by classical and simpler approaches. The development of an expression for the prefactor A_{ϵ_θ} of this power law is presented in §2.6. Models for the mixed velocity–temperature moments are then developed in §3 in order to propose a relatively simple expression (§4) for A_{ϵ_θ} ; we will show that this parameter is not universal since it is influenced by the boundary conditions of the jet. Finally, using these results, simple expressions are also presented in §4 for the turbulent Péclet number and the thermal-to-mechanical time scale ratio.

2. Outcomes of self-preservation for the scalar on the jet axis

2.1. Power-law evolution of ϵ_θ derived from the scale-by-scale budget

The analytical approach supporting the development of a power law expressing the longitudinal evolution of ϵ_θ is based on a self-preservation solution of the transport equation for $\overline{(\delta\theta)^2}$, the second-order temperature structure function; $\delta\theta = (\theta^+ - \theta)$, where $\theta^+ = \theta(x + s)$ and $\theta = \theta(x)$ depends on the separations s between two points along the jet axis. Starting from the temperature equation written at two independent points in space, and assuming local isotropy and local homogeneity (see Burattini *et al.* 2005a, for a discussion on the homogeneity condition), the transport equation for $\overline{(\delta\theta)^2}$ is written as:

$$-\overline{(\delta u)(\delta\theta)^2} + 2\alpha \frac{d\overline{(\delta\theta)^2}}{ds} + LST(s) = \frac{4}{3}\epsilon_\theta s, \quad (2.1)$$

where $LST(s)$ represents the contribution of the large scales to the budget of $\overline{(\delta\theta)^2}$. Here, similar developments to those reported by Antonia *et al.* (1997), Hill (1997, 2001), Danaïla *et al.* (1999), Shivamoggi & Antonia (2000) and Burattini, Antonia & Danaïla (2005*b*) are used to derive the large scale term on the jet axis:

$$LST(s) = -C(s) - P(s) - D(s), \tag{2.2}$$

where

$$C(s) = \frac{1}{s^2} U_0 \int_0^s y^2 \frac{\partial \overline{(\delta\theta)^2}}{\partial x} dy, \tag{2.3}$$

$$P(s) = \frac{2}{s^2} \frac{d\Theta_0}{dx} \int_0^s y^2 \overline{(\delta u)(\delta\theta)} dy, \tag{2.4}$$

$$D(s) = \frac{1}{2s^2} \int_0^s y^2 \frac{\partial}{\partial \bar{x}} \left[\overline{(u^+ + u)(\delta\theta)^2} \right] dy + \frac{4}{s^2} \int_0^s y^2 \frac{\partial}{\partial r} \overline{v(\delta\theta)^2} dy, \tag{2.5}$$

where $\bar{x} = x + s/2$ (\bar{x} being the midpoint), $\delta u = (u^+ - u)$, $u^+ = u(x + s)$ and $u = u(x)$. The three terms defined in (2.3) to (2.5), $C(s)$, $P(s)$ and $D(s)$, represent convection, production and turbulent diffusion, respectively. In the limit $s \rightarrow \infty$, equation (2.1) yields the one-point budget of $\overline{\theta^2}/2$, which is expressed (neglecting molecular diffusion) as

$$-U_0 \frac{\partial \overline{\theta^2}/2}{\partial x} - u\theta \frac{d\Theta_0}{dx} - \frac{1}{2} \frac{\partial u\theta^2}{\partial x} - \frac{\partial v\theta^2}{\partial r} \simeq \epsilon_\theta, \tag{2.6}$$

where Θ_0 is the local mean temperature excess relative to the ambient for $r = 0$. The first term on the left-hand side of this expression represents convection (C_θ), the second stands for production (P_θ) and the last two terms correspond to the longitudinal (D_{θ_x}) and radial (D_{θ_r}) contributions to the turbulent diffusion (D_θ). Darisse, Lemay & Benaïssa (2014) showed that D_{θ_r} is more than 300 times larger than D_{θ_x} on the jet axis. For the one-point budget, it is thus justified to neglect the longitudinal contribution from the turbulent diffusion term (see § 2.6). However, since this term is not necessarily negligible at all scales, we have included its contribution in the definition of $D(s)$ (2.5) in the sbs budget.

Self-preservation form of the equations (2.1)–(2.5) can be obtained when the different terms are expressed using the following functional forms (see Antonia *et al.* 2004; Burattini *et al.* 2005*b*)

$$\overline{(\delta\theta)^2} = \tilde{\theta}^2(x) h_\theta(s^*), \tag{2.7}$$

$$\overline{(\delta u)^2} = \tilde{u}^2(x) h_u(s^*), \tag{2.8}$$

$$\overline{(\delta u)(\delta\theta)} = \tilde{A}_\theta(x) a(s^*), \tag{2.9}$$

$$\overline{(\delta u)(\delta\theta)^2} = \tilde{B}_\theta(x) b_1(s^*), \tag{2.10}$$

$$\overline{(u^+ + u)(\delta\theta)^2} = \tilde{B}_\theta(x) b_2(s^*), \tag{2.11}$$

$$\overline{v(\delta\theta)^2} = \tilde{C}_\theta(x) c(s^*), \tag{2.12}$$

where $s^* \equiv s/l_\theta$, l_θ being the characteristic length scale for the temperature field. Note that the expression for $\overline{(\delta u)^2}$ is not directly related to (2.1)–(2.5), but it will be used later on, for the analysis of the mixed skewness increment. The scaling functions $\tilde{\theta}^2(x)$, $\tilde{u}^2(x)$, $\tilde{A}_\theta(x)$, $\tilde{B}_\theta(x)$, $\tilde{C}_\theta(x)$ characterize the streamwise evolution of the structure functions, while the dimensionless (s^*) functions represent the shape of

these structure functions. For the mixed velocity–temperature scales, as in Antonia *et al.* (2004), we avoid making the *a priori* assumption that these functions are represented by a combination of uncoupled velocity and temperature scales. For example, \tilde{A}_θ is a mixed scale with dimensions of velocity times temperature, but it is not *a priori* considered as being represented by the product of a velocity scale with a temperature scale.

Substitution of expressions (2.7)–(2.12) (in which we drop x and s^* for convenience) into (2.1) and dividing by $(\epsilon_\theta s^*)$ yields, after some manipulation,

$$\begin{aligned}
 & - \left[\frac{\tilde{B}_\theta}{l_\theta \epsilon_\theta} \right] \frac{b_1}{s^*} + \left[\frac{\alpha \tilde{\theta}^2}{l_\theta^2 \epsilon_\theta} \right] 2 \frac{dh_\theta}{ds^*} - \left[\frac{U_0}{\epsilon_\theta} \frac{d\tilde{\theta}^2}{dx} \right] \Gamma_1^* + \left[\frac{U_0 \tilde{\theta}^2}{l_\theta \epsilon_\theta} \frac{dl_\theta}{dx} \right] \Gamma_2^* - \left[\frac{\tilde{A}_\theta}{\epsilon_\theta} \frac{d\Theta_0}{dx} \right] \Gamma_3^* \\
 & + \left[\frac{\tilde{B}_\theta}{l_\theta \epsilon_\theta} \frac{1}{2} \frac{dl_\theta}{d\bar{x}} \right] \Gamma_4^* - \left[\frac{1}{\epsilon_\theta} \frac{d\tilde{B}_\theta}{d\bar{x}} \right] \Gamma_5^* - \left[\frac{\tilde{C}_\theta}{l_\theta \epsilon_\theta} \right] \Gamma_6^* = \left[\frac{4}{3} \right], \tag{2.13}
 \end{aligned}$$

where the functions Γ_i^* , which represent the shape functions of the large scale terms (LST), are expressed as

$$\Gamma_1^* = \frac{1}{s^{*3}} \int_0^{s^*} h_\theta y^{*2} dy^*, \tag{2.14}$$

$$\Gamma_2^* = \frac{1}{s^{*3}} \int_0^{s^*} \frac{dh_\theta}{dy^*} y^{*3} dy^*, \tag{2.15}$$

$$\Gamma_3^* = \frac{2}{s^{*2}} \int_0^{s^*} a y^{*2} dy^*, \tag{2.16}$$

$$\Gamma_4^* = \frac{1}{s^{*3}} \int_0^{s^*} \frac{db_2}{dy^*} y^{*3} dy^*, \tag{2.17}$$

$$\Gamma_5^* = \frac{1}{2s^{*3}} \int_0^{s^*} b_2 y^{*2} dy^*, \tag{2.18}$$

$$\Gamma_6^* = \frac{4}{s^{*3}} \int_0^{s^*} \frac{dc}{dy^*} \frac{\partial y^*}{\partial r^*} y^{*2} dy^*. \tag{2.19}$$

Self-preservation requires that all terms within brackets should evolve in x in exactly the same manner. Since the term on the right-hand side of (2.13) is constant, all the terms within brackets should be constant. This yields the following self-preservation constraints (where C_i are constants):

$$\left[\frac{\tilde{B}_\theta}{l_\theta \epsilon_\theta} \right] = C_1, \tag{2.20}$$

$$\left[\frac{\alpha \tilde{\theta}^2}{l_\theta^2 \epsilon_\theta} \right] = C_2, \tag{2.21}$$

$$\left[\frac{U_0}{\epsilon_\theta} \frac{d\tilde{\theta}^2}{dx} \right] = C_3, \tag{2.22}$$

$$\left[\frac{U_0 \tilde{\theta}^2}{l_\theta \epsilon_\theta} \frac{dl_\theta}{dx} \right] = C_4, \tag{2.23}$$

$$\left[\frac{\tilde{A}_\theta}{\epsilon_\theta} \frac{d\Theta_0}{dx} \right] = C_5, \tag{2.24}$$

$$\left[\frac{\tilde{B}_\theta}{l_\theta \epsilon_\theta} \frac{1}{2} \frac{dl_\theta}{d\bar{x}} \right] = \left[\frac{\tilde{B}_\theta}{l_\theta \epsilon_\theta} \frac{dl_\theta}{dx} \right] = C_6, \tag{2.25}$$

$$\left[\frac{1}{\epsilon_\theta} \frac{d\tilde{B}_\theta}{d\bar{x}} \right] = \left[\frac{2}{\epsilon_\theta} \frac{d\tilde{B}_\theta}{dx} \right] = C_7, \tag{2.26}$$

$$\left[\frac{\tilde{C}_\theta}{l_\theta \epsilon_\theta} \right] = C_8. \tag{2.27}$$

Following the definition of the midpoint \bar{x} , we can write $dl_\theta/d\bar{x} = dl_\theta/dx^+ + dl_\theta/dx$ (see for example Hill 2001; Danaila *et al.* 2012). Along the jet axis, in the far field, it is considered that $dl_\theta/dx = dl_\theta/dx^+$, and the derivative in C_6 has been written as $dl_\theta/d\bar{x} = 2dl_\theta/dx$. The same reasoning applies to the derivative of \tilde{B}_θ involved in C_7 .

Manipulation of C_i constants yields the following constraints:

$$\frac{C_6}{C_1} = \frac{dl_\theta}{dx}, \tag{2.28}$$

$$\frac{C_1 C_4}{C_2 C_6} = \frac{U_0 l_\theta}{\alpha}, \tag{2.29}$$

$$\frac{C_5 C_6}{C_1 C_4} = \frac{\tilde{A}_\theta l_\theta}{U_0 \tilde{\theta}^2} \frac{d\Theta_0}{dx}, \tag{2.30}$$

$$\frac{C_6}{C_4} = \frac{\tilde{B}_\theta}{U_0 \tilde{\theta}^2}, \tag{2.31}$$

$$\frac{C_1}{C_8} = \frac{\tilde{B}_\theta}{\tilde{C}_\theta}. \tag{2.32}$$

The two first constraints allow us to write $l_\theta \propto \hat{x}$ and, for a given value of α , $U_0 \propto \hat{x}^{-1}$. It is worth mentioning that the usual power law for U_0 , *viz.* $U_0/U_j = B_U \hat{x}^{-1}$, is more formally obtained here than the one resulting from the momentum equation.

In addition, the self-preservation analysis of the mean temperature equation presented in § A.1 strictly shows that Θ_0 , scales with \hat{x}^{-1} (yielding $d\Theta_0/dx \propto \hat{x}^{-2}$). This self-preservation analysis also shows, from (A 11), that $H_0 \propto \hat{x}^{-2}$ (H_0 represents $\overline{u\theta}$ on the jet axis). It is thus required that \tilde{A}_θ has to scale with \hat{x}^{-2} , because $\tilde{A}_\theta = 2H_0$ when $s \rightarrow \infty$.

Using the power laws just derived, *viz.* $l_\theta \propto \hat{x}$, $U_0 \propto \hat{x}^{-1}$, $\tilde{A}_\theta \propto \hat{x}^{-2}$ and $d\Theta_0/dx \propto \hat{x}^{-2}$ into constraint (2.30) yields

$$\tilde{\theta}^2 \propto \frac{\tilde{A}_\theta l_\theta}{U_0} \frac{d\Theta_0}{dx} \propto \hat{x}^{-2}. \tag{2.33}$$

Finally, introducing $d\Theta_0/dx \propto \hat{x}^{-2}$ and $\tilde{A}_\theta \propto \hat{x}^{-2}$ into expression (2.24), which defines the fifth constraint C_5 , yields the -4 th power law for ϵ_θ :

$$\epsilon_\theta \propto \hat{x}^{-4}. \tag{2.34}$$

This expression is similar to the -4 th power law previously derived by TAD and DALL for ϵ_k . The mean dissipation rate of $\overline{\theta^2}/2$, normalized by the jet exit parameters, can finally be written as

$$\frac{\epsilon_\theta D}{U_j \Theta_j^2} = A_{\epsilon_\theta} \hat{x}^{-4}. \quad (2.35)$$

In the context of complete self-preservation, it should be noted that other velocity scales, like ν_K or $\sqrt{\overline{u^2}}$ could have been used, interchangeably, instead of U_0 (see Burattini *et al.* 2005b, and TAD), as far as the chosen velocity scales with \hat{x}^{-1} . The same reasoning applies to the temperature scale. For example, the Kolmogorov temperature $\theta_K \equiv (\epsilon_\theta \eta / \nu_K)^{1/2}$, which scales with \hat{x}^{-1} , could have been used, interchangeably, instead of Θ_0 .

Moreover, should \tilde{A}_θ , defined in relation (2.9), have been *a priori* expressed as the product of uncoupled velocity and temperature scales, the same final result would have been obtained in a simpler way, by the sole use of the sbs budget. We however prefer to avoid this assumption and use the mean temperature equation to close the problem.

2.2. Power laws for temperature variance and mixed moments

Under the assumption of local homogeneity, the temperature variance can be defined as half the temperature structure function considered for large separations, *viz.* $\overline{\theta^2} = (\overline{\delta\theta})^2/2$ (for $s \rightarrow \infty$). From the previous developments, it follows immediately that $\overline{\theta^2} \propto \Theta_0^2 \propto \hat{x}^{-2}$. We thus introduce the parameter

$$B_I^2 = \frac{\overline{\theta^2}}{\Theta_0^2}, \quad (2.36)$$

which must be constant along the jet axis. The term B_I for the temperature field is comparable to the parameter $A_I = \overline{u^2}/U_0^2$ introduced by TAD for the velocity field. Darisse *et al.* (2015) observed in their jet that B_I was constant for $\hat{x} > 20$. For the slightly heated round jet studied by Darisse *et al.* (2015), the longitudinal distributions of R_U , U_0 , Θ_0 , $\overline{u^2}$, $\overline{\theta^2}$ and ϵ_θ , all normalized by the jet exit parameters, are presented in figure 1. All these quantities share the same virtual origin $x_0 = 1.65$ which has been obtained from least-square regressions performed over the whole dataset related to the self-preserving region. The log–log scale highlights the power-law behaviour of these quantities. The location corresponding to the self-preserving region depends on the quantity of interest, but it is shown that full self-preservation is clearly reached for $\hat{x} > 30$. Table 1 presents the power-law equation used for each quantity and the (measured) value of their corresponding power-law coefficients.

Recalling from expression (2.9) that \tilde{A}_θ has the dimensions of velocity times temperature and that $\tilde{A}_\theta \propto \hat{x}^{-2}$, it immediately follows that, along the jet axis,

$$\tilde{A}_\theta \propto U_0 \Theta_0 \propto \tilde{u} \tilde{\theta} \propto \hat{x}^{-2}, \quad (2.37)$$

where $\tilde{u} \propto \hat{x}^{-1}$ is a characteristic velocity scale (see (2.8)) used by DALL in their sbs analysis of the energy equation. Relation (2.37) indicates that \tilde{A}_θ (a mixed velocity–temperature scale) is finally expressed as the product of uncoupled velocity and temperature scales. This also reveals that the normalized longitudinal temperature flux $u\theta/(U_0\Theta_0)$ is constant along the jet axis.

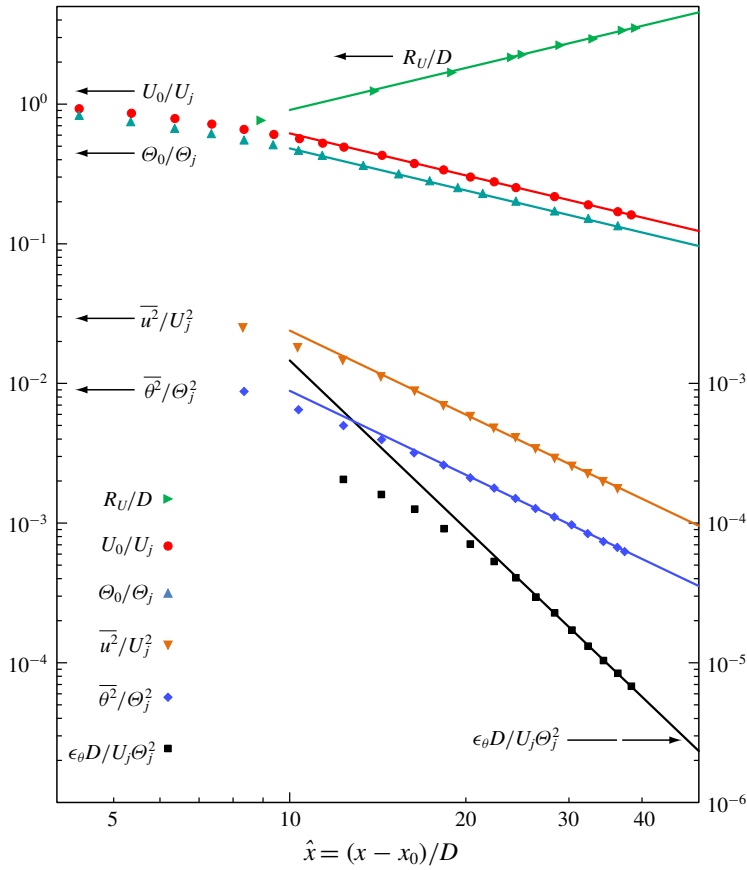


FIGURE 1. (Colour online) Streamwise evolution of R_U/D , U_0/U_j , Θ_0/Θ_j , $\overline{u^2}/U_j^2$, $\overline{\theta^2}/\Theta_j^2$ and $\epsilon_\theta D/(U_j\Theta_j^2)$ along the jet axis (symbols) and their corresponding power laws (measurements of Darisse, Lemay & Benaïssa 2013a,b; Darisse *et al.* 2015).

Power laws	Coefficients
$R_U/D = B_{R_U}\hat{x}$	$B_{R_U} = 0.091$
$U_0/U_j = B_U\hat{x}^{-1}$	$B_U = 6.171$
$\Theta_0/\Theta_j = B_\Theta\hat{x}^{-1}$	$B_\Theta = 4.819$
$\overline{u^2}/U_j^2 = A_U^2 B_U^2 \hat{x}^{-2}$	$A_U^2 B_U^2 = 2.389$ ($A_U = 0.2505$)
$\overline{\theta^2}/\Theta_j^2 = B_\Theta^2 B_\Theta^2 \hat{x}^{-2}$	$B_\Theta^2 B_\Theta^2 = 0.886$ ($B_\Theta = 0.1953$)
$\epsilon_\theta D/(U_j\Theta_j^2) = A_{\epsilon_\theta}\hat{x}^{-4}$	$A_{\epsilon_\theta} = 14.583$

TABLE 1. Definition of the power laws shown in figure 1 and obtained from the measurements of Darisse *et al.* (2015) ($Re_D = 1.4 \times 10^5$, $Re_\lambda = 548$ and $Pe_\lambda = 211$).

The temperature scale is now introduced into relations (2.31) and (2.32) which leads to

$$\tilde{B}_\theta \propto \tilde{C}_\theta \propto U_0 \Theta_0^2 \propto \hat{x}^{-3}. \tag{2.38}$$

These mixed velocity–temperature scales are both represented by the product of an uncoupled velocity scale and a temperature squared scale. The above relations also indicate that the normalized mixed moments, $\overline{u\theta^2}/(U_0\Theta_0^2)$ and $\overline{v\theta^2}/(U_0\Theta_0^2)$, are constant along the jet axis. This also allows the mixed skewness increment to be expressed as:

$$S_\theta = \frac{\overline{(\delta u)(\delta\theta)^2}}{(\overline{\delta u})^{2^{1/2}}(\overline{\delta\theta})^2} = \frac{\tilde{B}_\theta}{\tilde{u}\tilde{\theta}^2} \frac{b_1(s^*)}{h_u(s^*)h_\theta(s^*)} = c_S\phi_\theta(s^*). \quad (2.39)$$

The power laws for \tilde{B}_θ , \tilde{u} and $\tilde{\theta}^2$ indicate that the scaling function c_S is constant. This direct consequence of self-preservation on the jet axis was also observed for the velocity field by DALL. They have shown that c_q , the scaling function of the mixed skewness increment of velocity and kinetic energy, was constant.

2.3. Turbulent Péclet number along the jet axis

Another outcome of this analysis pertains to the evolution of the turbulent Péclet number ($Pe_\lambda \equiv \sqrt{u^2}\lambda_\theta/\alpha$, where $\lambda_\theta \equiv \sqrt{3\alpha\overline{\theta^2}/\epsilon_\theta}$). Considering that $\overline{\theta^2} \propto \hat{x}^{-2}$ and $\epsilon_\theta \propto \hat{x}^{-4}$, it follows immediately that $\lambda_\theta \propto \hat{x}$. Recalling that $\sqrt{u^2} \propto \hat{x}^{-1}$, one concludes that the turbulent Péclet number must be constant along the jet axis in the self-preserving region. This behaviour was observed by Darisse *et al.* (2015) in their jet where Pe_λ was observed to be constant for $\hat{x} > 30$.

2.4. Characteristic length scales

The self-preservation analyses of the sbs budget revealed that the characteristic length scale of the temperature field evolves linearly, *viz.* $l_\theta \propto \hat{x}$, as indicated by (2.28). Thus, any length scale evolving linearly along the jet axis would be a relevant normalization length scale, for all scales, including those corresponding to the sufficiently large values of s , where the sbs budget yields the one-point $\overline{\theta^2}/2$ budget. It has been shown by Burattini *et al.* (2005*b*) and more rigorously by DALL that the Taylor and Kolmogorov microscales, *viz.* λ and η , can be used interchangeably, as these quantities both evolve linearly along the jet axis. Moreover, it was shown, in the previous section, that λ_θ also fulfils the requirements ensuing from the present self-preservation analysis. Finally, from § A.2, it is shown that R_U and R_θ , the half-radii of the mean velocity and temperature profiles, respectively, evolve linearly in the streamwise direction. Thus, η , λ , λ_θ , R_U and R_θ are all relevant quantities which could be used as an appropriate characteristic length scale. Hereafter, R_U is used (among the other relevant options) as the local normalization length scale.

2.5. Structure functions of temperature fluctuations

Further evidence of complete self-preservation can be inferred from the analysis of the temperature structure functions. Indeed, an indicator showing the fulfilment of complete self-preservation is obtained when the structure functions measured at several positions along the jet axis all collapse over the entire range of the increment s or scales, regardless of which set of scaling variables (complying with self-preservation conditions) is used for the normalization. In the present case, the second- and third-order structure functions for the temperature are considered.

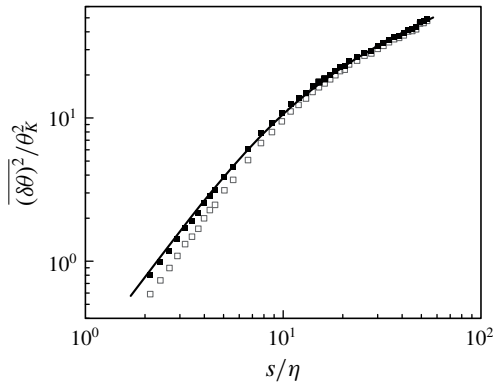


FIGURE 2. Second-order structure function of temperature fluctuations on the jet axis, at $x/D=30$, normalized with Kolmogorov scales θ_K and η (flow conditions similar to those of Darisse *et al.* 2013a,b, 2015). Symbols: measurements performed using two cold-wire probes separated by a distance s in the streamwise direction; open symbols: raw data; closed symbols: signals compensated for the attenuation resulting from the wire time constant (see Lemay & Benaïssa 2001; Lemay, Benaïssa & Antonia 2003; Darisse *et al.* 2014). Line: measurements performed using one cold-wire probe (compensated signal) and the assumption of Taylor's hypothesis ($s = \tau U_0$, where τ is the time increment).

Before considering the collapse of these structure functions along the jet axis, we first consider some technical aspects regarding their measurement, namely the effect of the limited time constant of the cold-wire probe and the validation of Taylor's hypothesis used to evaluate these functions. For that purpose, figure 2 shows the distribution of $\overline{(\delta\theta)^2}/\theta_K^2$ (Kolmogorov scaling) measured at a streamwise position $x/D=30$ on the jet axis. At this position, the ratio between the wire cutoff frequency and the Kolmogorov frequency is $f_c/f_K=0.7$. The attenuation of the cold-wire signal thus needs to be compensated and this is particularly important at small scales. The compensation of the cold-wire response is performed using the numerical processing technique proposed by Lemay & Benaïssa (2001), Lemay *et al.* (2003). The open and closed symbols in figure 2 show respectively the uncompensated and compensated distributions of $\overline{(\delta\theta)^2}/\theta_K^2$ obtained from the measurement of two distinct cold-wire probes separated by a distance s along the longitudinal direction. The effect of the compensation procedure is clearly seen at small scales. The full line represents the distribution of compensated $\overline{(\delta\theta)^2}/\theta_K^2$ inferred from a single cold-wire probe using Taylor's hypothesis. The time increment τ is converted to spatial separation s using a constant convection velocity, constant for all scales, defined by the mean streamwise velocity on the jet axis ($s = \tau U_0$). The agreement between the full line and the closed symbols in figure 2 indicates that the use of Taylor's hypothesis is thoroughly validated.

Hereinafter, the distributions of temperature structure functions measured at several positions along the jet axis ($x/D = 30$ to 60) are those obtained using Taylor's hypothesis and compensated signals. For the locations $x/D = 30, 35, 40, 45, 50, 55$ and 60, the ratio of the cutoff to the Kolmogorov frequencies evolves respectively from $f_c/f_K = 0.7, 0.9, 1.2, 1.4, 1.7, 2.1$ to 2.4. Thus, the use of the compensation procedure is mandatory for $x/D = 30$, but it becomes less important as one moves downstream to $x/D = 60$. Nevertheless, the compensation technique is applied to the temperature signals for all the measurement locations.

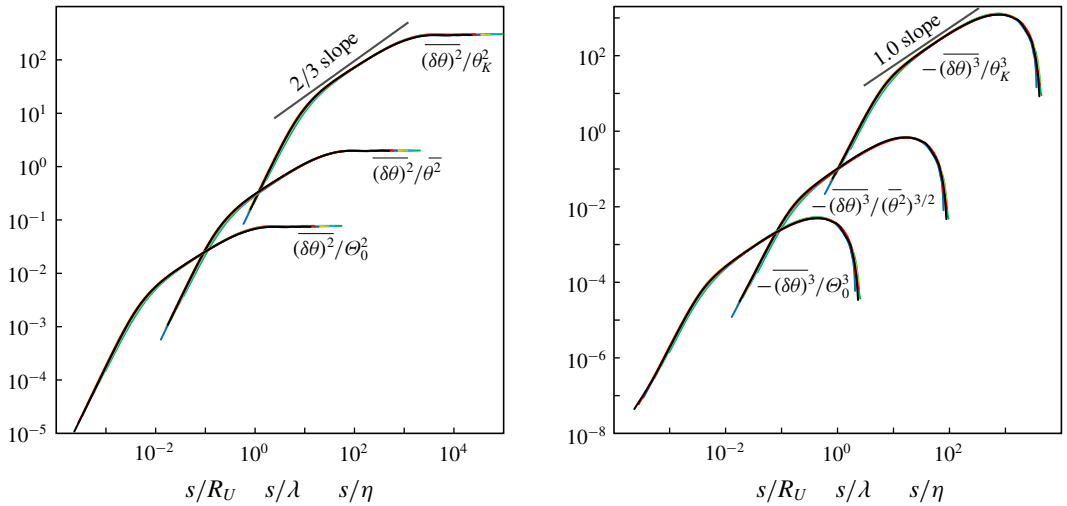


FIGURE 3. (Colour online) Temperature structure functions $\overline{(\delta\theta)^2}$ and $-\overline{(\delta\theta)^3}$ on the jet axis at 7 streamwise locations extending from $x/D = 30$ to 60, in steps of 5; normalization with θ_K and η (top), $\bar{\theta}^2$ and λ (centre), Θ_0 and R_U (bottom); flow conditions similar to those of Darisse *et al.* (2013a,b, 2015).

Figure 3 shows the distribution of the normalized second- and third-order temperature structure functions measured on the jet axis in the range $30 \leq x/D \leq 60$. Three different sets of scaling variables are used for normalization, *viz.* Kolmogorov scales (θ_K and η), Taylor scales ($\bar{\theta}^2$ and λ) and large scales (Θ_0 and R_U). Regardless of the normalization, both the second- and third-order temperature structure functions present a very good collapse over the entire range of scales for all the positions in the range $x/D = 30$ to 60. This indicates that complete self-preservation is satisfied for these positions on the jet axis, reinforcing confidence in the analytical development and results presented in § 2.1. Note that despite the moderately large value of Re_λ ($= 548$), $\overline{(\delta\theta)^2}$ does not strictly present a power-law variation of the form r^{ζ_2} in the scaling range. However, the figure suggests that increasing Re_λ would eventually lead to ζ_2 approaching the value ($\zeta_2 = 2/3$) predicted by Yaglom (1949). Note that nothing can be said about $-\overline{(\delta\theta)^3}$ which should not be confused with $-\overline{\delta u(\delta\theta)^2}$ for which the exponent $\zeta_3 = 1$ if there is an inertial range. If $-\overline{(\delta\theta)^3}$ is assumed to follow a power-law variation r^ζ in the inertial range, its power-law exponent is yet to be determined. Interestingly, the data suggest that as Re_λ increases ζ is likely to approach 1, a result which can be also observed in the data of Antonia & Van Atta (1978) (see their figures 1 and 2).

2.6. One-point $\bar{\theta}^2/2$ budget

As previously pointed out, Darisse *et al.* (2014) have shown that the one-point $\bar{\theta}^2/2$ budget on the jet axis is dominated by convection, production, the radial component of turbulent diffusion and dissipation. Their budget was evaluated in the self-preserving region since they showed that both Re_λ and Pe_λ were constant along the jet axis. Retaining only these predominant terms and recalling that outer scales U_0 , Θ_0 and R_U are relevant self-preservation scales, the normalized one-point budget on the jet

axis is written as (see Darisse *et al.* 2015, for details):

$$\epsilon_\theta^* = \frac{\epsilon_\theta R_U}{U_0 \Theta_0^2} \simeq B_{R_U} \frac{\overline{\theta^2}}{\Theta_0^2} + B_{R_U} \frac{\overline{u\theta}}{U_0 \Theta_0} - \frac{d}{d\xi} \left(\frac{\overline{v\theta^2}}{U_0 \Theta_0^2} \right) \simeq C_\theta^* + P_\theta^* + D_\theta^*, \quad (2.40)$$

where $\xi = r/R_U$ is the normalized radial coordinate. The power laws for ϵ_θ , R_U , U_0 and Θ_0 allow the dissipation term to be written as

$$\epsilon_\theta^* = \frac{A_{\epsilon_\theta} B_{R_U}}{B_U B_\Theta^2}. \quad (2.41)$$

Introducing this expression and the definition of B_I (2.36) into the normalized budget (2.40) and solving for A_{ϵ_θ} yields

$$A_{\epsilon_\theta} \simeq B_U B_\Theta^2 \left[B_I^2 + \frac{\overline{u\theta}}{U_0 \Theta_0} - \frac{1}{B_{R_U}} \frac{d}{d\xi} \left(\frac{\overline{v\theta^2}}{U_0 \Theta_0^2} \right) \right]. \quad (2.42)$$

This expression for the prefactor of the ϵ_θ power law (2.34) is more involved than its counterpart for ϵ_k , i.e. equation (1.2). The two mixed velocity–temperature moments accounting for the production and turbulent diffusion terms of the $\overline{\theta^2}/2$ budget add a level of complexity rendering this relation less attractive, from a modelling point of view, than the expression for A_{ϵ_k} . In the following section, we propose preliminary models for the longitudinal evolution of $\overline{u\theta}$ and $\overline{v\theta^2}$ along the jet axis. This will help us develop an ‘empirical’ expression for the prefactor A_{ϵ_θ} that will account for the effect of the jet boundary conditions and that can be estimated from relatively simple measurements.

3. Modelling the mixed velocity–temperature moments

3.1. Longitudinal velocity–temperature correlation model

The correlation $\overline{u\theta}$ is modelled by assuming weak anisotropy of the temperature field in the self-preserving region of the jet. This hypothesis applied to the scalar flux underpins the development of the well-known algebraic second moment closure for the scalar transport (see for example Gibson & Launder 1976; Hanjalić & Launder 2011). In the present case, this means that the ratio $\overline{u\theta}/\sqrt{k\theta^2}$ is expected to be constant. The approach can be simplified further by considering that the correlation coefficient $\rho_{u\theta} = \overline{u\theta}/\sqrt{\overline{u^2}\overline{\theta^2}}$ is constant across the jet width. The data reported by Darisse *et al.* (2015) ($x/D = 30$) and Chevray & Tutu (1978) ($x/D = 15$) indicate that $\rho_{u\theta}(r)$ does not vary significantly ($0.46 < \rho_{u\theta} < 0.51$) around the centreline. Pietri, Amielh & Anselmet (2000) made the same observation in a coflowing jet exiting from a pipe. They also showed that, along the centreline, in the region $15 \geq x/D \geq 28$, the value of $c_{u\theta}$ ($\equiv \rho_{u\theta}$ at $r = 0$) was almost constant. More precisely, $c_{u\theta}$ decreased slightly between 0.52 at $x/D = 15$ and 0.49 at $x/D = 28$. Their measurements are consistent with the value of 0.48 found here. Using a combination of laser-induced fluorescence and laser Doppler anemometry (LDA) techniques in a slightly heated water jet, Lemoine *et al.* (1999) reported a measured value of $c_{u\theta} = 0.48$, which also confirms the validity of the present value. Finally, additional support is obtained with the results presented by Panchapakesan & Lumley (1993b) in a helium jet. From their reported longitudinal

evolution of $\sqrt{\overline{u^2}}$ on the centreline, we can extrapolate this quantity up to the far non-buoyant region and find that, for this flow configuration too, $c_{u\theta} = 0.48$.

Based on these reported observations, the following model is adopted on the jet axis:

$$\overline{u\theta} = c_{u\theta} \sqrt{\overline{u^2\theta^2}} \quad \text{with } c_{u\theta} = \rho_{u\theta}(r=0) = 0.48. \quad (3.1)$$

This expression is also a direct consequence of the self-preservation analysis performed on the sbs budget in § 2.1. It is shown that, along the jet axis, $\overline{u\theta} \propto \hat{x}^{-2}$ (see also expression (A 11)), $\sqrt{\overline{u^2}} \propto \hat{x}^{-1}$ and $\sqrt{\overline{\theta^2}} \propto \hat{x}^{-1}$; it immediately follows that $\rho_{u\theta}$ is constant along the jet axis. Darisse *et al.* (2015) showed that Re_λ and Pe_λ are constant along the jet axis, and concluded that complete self-preservation for the velocity and the scalar fields was satisfied. Thus, based on their measurements, $c_{u\theta} = 0.48$ is adopted in (3.1) for $\overline{u\theta}$. Introducing the previously defined coefficients terms A_I and B_I , the model for the normalized mixed correlation is written as

$$\frac{\overline{u\theta}}{U_0\Theta_0} = c_{u\theta}A_I B_I \quad \text{with } c_{u\theta} = 0.48. \quad (3.2)$$

3.2. Turbulent diffusion model

Using the transport equation of $\overline{u_i\theta^2}$ in which the convective transport was neglected, Dekeyser & Launder (1983) proposed a model based on a Gaussian approximation for the fourth-order moments and a return-to-isotropy representation for pressure interactions:

$$\overline{u_i\theta^2} = -c_\theta \frac{k}{\epsilon_k} \left(\overline{u_i u_j} \frac{\partial \overline{\theta^2}}{\partial x_j} + 2\overline{u_i\theta} \frac{\partial \overline{u_j\theta}}{\partial x_j} \right) \quad \text{with } c_\theta = 0.11. \quad (3.3)$$

When the last term on the right-hand side of relation (3.3) is omitted, the truncated expression represents the simple gradient-type model widely used in numerical calculations. As reported by Dekeyser & Launder (1983), this truncation is usually made to facilitate numerical solutions. They, however, mentioned that the complete form was in better agreement with their measurements. In the present case, we are interested in the radial component of (3.3) which is explicitly expressed as

$$\overline{v\theta^2} = -c_\theta \frac{k}{\epsilon_k} \left[\overline{uv} \frac{\partial \overline{\theta^2}}{\partial x} + \overline{v^2} \frac{\partial \overline{\theta^2}}{\partial r} + 2\overline{v\theta} \left(\frac{\partial \overline{u\theta}}{\partial x} + \frac{\partial \overline{v\theta}}{\partial r} \right) \right]. \quad (3.4)$$

The terms involving longitudinal derivatives are relatively small compared to the two other terms within the brackets, particularly in the mid and far fields. The measurements reported by Darisse *et al.* (2015) indicate that the longitudinal derivative terms represent approximately -16% of the radial derivative contributions. To simplify the model, the longitudinal derivative terms are omitted and, to compensate for the effect of this omission, the value of c_θ is reduced by 16% to 0.095. This yields a simplified model:

$$\overline{v\theta^2} \simeq -c_\theta \frac{k}{\epsilon_k} \left[\overline{v^2} \frac{\partial \overline{\theta^2}}{\partial r} + 2\overline{v\theta} \frac{\partial \overline{v\theta}}{\partial r} \right]. \quad (3.5)$$

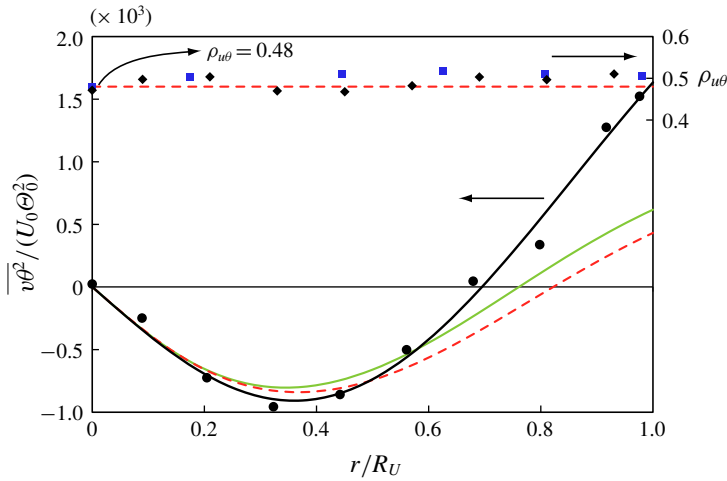


FIGURE 4. (Colour online) Radial distributions of normalized velocity–temperature moments near the jet axis; right side, correlation coefficient $\rho_{u\theta}$: Darisse *et al.* (2015) (black diamonds), Chevray & Tutu (1978) (blue squares) and model defined by (3.1) (red dashed line); left scale, $\overline{v\theta^2}/(U_0\theta_0^2)$: Darisse *et al.* (2015) (black circles) with best fit (black line), model of Dekeyser & Launder (1983), equation (3.4), (green line) and simplified model defined by (3.5) (red dashed line).

The database of Darisse *et al.* (2015) is used here to test the validity of these models on the jet axis. All the radial distributions of the measured quantities reported by these authors have been fitted with least-square regressions using the mathematical expressions given in Hussein, Capp & George (1994). Near the jet axis ($r/R_U \leq 0.5$), figure 4 indicates that both, relations (3.4) and (3.5) are in good agreement with the measurements of $\overline{v\theta^2}/(U_0\theta_0^2)$. Moreover, very close to the centreline (around $r/R_U \leq 0.2$), simplified and Dekeyser–Launder models are almost perfectly equivalent. As the present development focuses on the evolution of different quantities on the centreline, the simplified model (3.5) is used. The radial derivative of $\overline{v\theta^2}$, which represents the dominant part of the turbulent diffusion of $\overline{\theta^2}/2$ on the jet axis (where $\overline{v\theta} \equiv 0$ and $\partial\overline{\theta^2}/\partial r \equiv 0$ on the axis by virtue of axisymmetry), is written as

$$\frac{\partial\overline{v\theta^2}}{\partial r} \simeq -c_\theta \frac{k}{\epsilon_k} \left[\overline{v^2} \frac{\partial^2\overline{\theta^2}}{\partial r^2} + 2 \left(\frac{\partial\overline{v\theta}}{\partial r} \right)^2 \right]. \tag{3.6}$$

The data of Darisse *et al.* (2015) reveal that the two terms within brackets are approximately equal. Thus, we can write (3.6) as follows

$$\frac{\partial\overline{v\theta^2}}{\partial r} \simeq -4c_\theta \frac{k}{\epsilon_k} \left(\frac{\partial\overline{v\theta}}{\partial r} \right)^2. \tag{3.7}$$

The radial gradient of $\overline{v\theta}$ on the jet axis can be obtained directly from the mean temperature equation, after neglecting $\partial\overline{u\theta}/\partial x$ and the molecular diffusion term, *viz.*

$$\frac{\partial\overline{v\theta}}{\partial r} \simeq -\frac{1}{2} U_0 \frac{d\theta_0}{dx}. \tag{3.8}$$

The combination of (3.7) and (3.8) yields, on the jet axis, a model for the turbulent diffusion of $\overline{\theta^2}/2$

$$\frac{\partial \overline{v\theta^2}}{\partial r} \simeq -c_\theta \frac{k}{\epsilon_k} U_0^2 \left(\frac{d\Theta_0}{dx} \right)^2 \quad \text{with } c_\theta = 0.095. \quad (3.9)$$

Using relation (A 17) for the streamwise gradient of Θ_0 , the normalized form of this model is

$$\frac{d}{d\xi} \left(\frac{\overline{v\theta^2}}{U_0 \Theta_0^2} \right) \simeq -c_\theta B_{RU}^2 \frac{k}{U_0^2} \frac{U_0^3}{\epsilon_k R_U}. \quad (3.10)$$

Introducing the notation $k/U_0^2 = A_I^2 (\mathcal{R} + 1/2)$ and relation (1.3), which represents ϵ_k^* , yields the final form of the normalized turbulent diffusion model:

$$\frac{d}{d\xi} \left(\frac{\overline{v\theta^2}}{U_0 \Theta_0^2} \right) \simeq -c_\theta B_{RU} \frac{(\mathcal{R} + 1/2)}{(\mathcal{R} + 2)} \quad \text{with } c_\theta = 0.095. \quad (3.11)$$

4. Outcomes related to the dissipation

4.1. Mean dissipation rate of $\overline{\theta^2}/2$

The models for the mixed correlation (3.2) and the turbulent diffusion (3.11) introduced into relation (2.42) allow an empirical expression for the prefactor A_{ϵ_θ} to be obtained:

$$A_{\epsilon_\theta} \simeq B_U B_\theta^2 \left[B_I^2 + c_{u\theta} A_I B_I + c_\theta \left(\frac{\mathcal{R} + 1/2}{\mathcal{R} + 2} \right) \right], \quad (4.1)$$

with $c_{u\theta} = 0.48$, $c_\theta = 0.095$. Using the data of Darisse *et al.* (2015) expression (4.1) yields $A_{\epsilon_\theta} = 15.02$. This is in very good agreement with the value $A_{\epsilon_\theta} = 14.58$ obtained from the measurements presented in figure 1. It is important to note that the coefficient $A_{\epsilon_\theta} = 14.58$ was obtained from the power law of ϵ_θ shown in figure 1. The values of ϵ_θ were estimated from the integral of the dissipation spectra of temperature fluctuations, under the assumption of local isotropy and Taylor's hypothesis. It was shown by Darisse *et al.* (2015) that, at $\hat{x} = 30$, the isotropic estimate of ϵ_θ on the jet centreline was in very good agreement with the value inferred from the balance of the temperature budget. Therefore, this value of 14.58 was evaluated from a dataset different than the one used to evaluate $A_{\epsilon_\theta} = 15.02$ with expression (4.1). This guarantees that the validation of the empirical expression is made using an independent test.

After inserting (4.1) into (2.41), ϵ_θ normalized with local outer scales, R_U , U_0 and Θ_0 , can be expressed as:

$$\epsilon_\theta^* \simeq B_{RU} \left[B_I^2 + c_{u\theta} A_I B_I + c_\theta \left(\frac{\mathcal{R} + 1/2}{\mathcal{R} + 2} \right) \right]. \quad (4.2)$$

By virtue of (2.40), expression (4.2) also defines a simple empirical expression for the dissipation of $\overline{\theta^2}/2$ on the jet axis. The validity of this empirical expression for ϵ_θ^* has been tested using four datasets (see table 2). We have to point out that

	DLB	AM	PL	RAL
Re_D	140 000	19 000	4000	256 000
B_U	6.171	5.6	6.5	5.0
B_{R_U}	0.091	0.099	0.116	0.100
A_I	0.2505	0.2600	0.3300	0.2900
\mathcal{R}	0.7516	0.4793	0.3492	0.5600
B_I	0.1953	0.2000	0.1950	0.1700
$\epsilon_\theta R_U / (U_0 \Theta_0^2)$ (meas. or simul.)	0.00955	0.00966	0.0114	0.0105
$\epsilon_\theta R_U / (U_0 \Theta_0^2)$ from (4.2)	0.00952	0.0101	0.0120	0.0092
Deviation from meas. or simul.	-0.3 %	+5.0 %	+5.1 %	-12.5 %
Pe_λ (meas. or simul.)	211	83	48.3	251.2
Pe_λ from (4.5)	205	77.3	47.1	268.5
Deviation from meas. or simul.	-2.8 %	-6.8 %	-2.4 %	+6.9 %

TABLE 2. Estimates obtained from the simple empirical expressions compared with the results presented by Darisse *et al.* (2015) (DLB, measurements in a heated jet), Antonia & Mi (1993) (AM, measurements in a heated jet), Panchapakesan & Lumley (1993*b*) (PL, measurements in the non-buoyant region of a helium jet) and Ruffin *et al.* (1994) (RAL, simulations using second-order turbulence models with a passive scalar).

very few datasets in the literature provide measurements for ϵ_θ^* in a well-established self-similar region of a slightly heated turbulent round jet. As already mentioned, Darisse *et al.* (2015) reported such measurements (inferred from the $\overline{\theta^2}/2$ budget and locally isotropic estimates). In their case, the outcome of the empirical expression (4.2) differs by only -0.3 % from their measurement. Antonia & Mi (1993) presented direct measurements and locally isotropic estimates for ϵ_θ^* (which were in agreement on the jet centreline) in a slightly heated round jet in the region $\hat{x} = 15$. The outcome of relation (4.2) differs by +5 % from their measurement. This is in rather good agreement considering that, in their case, self-similarity is probably not completely achieved at $\hat{x} = 15$. The third dataset was provided by Panchapakesan & Lumley (1993*b*) which reported measurements (inferred from the budget of the variance of concentration fluctuations) in the non-buoyant region of a helium round jet. Considering that this flow field shows some analogies with the present case, it is interesting to observe that the outcome of relation (4.2) differs by only +5.1 % from their measurement. Finally, the Reynolds-averaged Navier–Stokes (RANS) simulations reported by Ruffin *et al.* (1994) (air jet with a passive contaminant) were used to provide a computational fluid dynamics (CFD) test case. The value of ϵ_θ^* calculated with expression (4.2) differs by -12.5 % from their simulation on the jet centreline. Considering that RANS simulations of turbulent round jets are usually not in perfect concordance with the measurements (as reported by these authors), the present level of agreement is rather satisfactory.

4.2. Turbulent Péclet number

It was shown in § 2.3 that the turbulent Péclet number Pe_λ , which can be expressed as

$$Pe_\lambda = \sqrt{\frac{3\overline{u^2\theta^2}}{\alpha\epsilon_\theta}}, \quad (4.3)$$

is constant along the jet axis. The power laws for $\overline{u^2}$, $\overline{\theta^2}$ and ϵ_θ are now introduced in order to express Pe_λ as follows

$$Pe_\lambda = A_I B_I B_U B_\Theta \sqrt{\frac{3Re_D Pr}{A_{\epsilon_\theta}}}, \quad (4.4)$$

where $Pr \equiv \alpha/\nu$, the Prandtl number, is considered to be equal to 0.71. Using (4.1), the final expression for Pe_λ is

$$Pe_\lambda = A_{pe} \sqrt{Re_D Pr} = \left[A_I B_I \sqrt{\frac{3B_U}{B_I^2 + c_{u\theta} A_I B_I + c_\theta \frac{(\mathcal{R} + 1/2)}{(\mathcal{R} + 2)}}} \right] \sqrt{Re_D Pr}. \quad (4.5)$$

Since the prefactor A_{pe} (term in brackets), depends on B_U , A_I , B_I and \mathcal{R} , a set of parameters influenced by the jet boundary conditions, its value is likely to depend on the initial/boundary conditions. However, equation (4.5) gives $A_{pe} = 0.66$ and 0.71 for the Darisse *et al.* (2015) and Antonia & Mi (1993) data respectively. It appears that the boundary conditions do not severely impact this parameter. Thus, it seems reasonable to use an average – and constant – value of $A_{pe} = 0.68$. With this assumption, relation (4.5) yields $Pe_\lambda = 211$ for Darisse *et al.* (2015) and 79 for Antonia & Mi (1993), which results are in good agreement with the measurements.

4.3. Thermal-to-mechanical time scale ratio

The thermal-to-mechanical time scale ratio is defined as

$$R = \frac{\overline{\theta^2}/(2\epsilon_\theta)}{k/\epsilon_k}. \quad (4.6)$$

Using the different power laws derived here for the physical quantities involved in this expression allows the following simple model on the jet axis to be written as

$$R \simeq \frac{B_I^2 (\mathcal{R} + 2)}{\left(B_I^2 + c_{u\theta} A_I B_I + c_\theta \frac{(\mathcal{R} + 1/2)}{(\mathcal{R} + 2)} \right) (2\mathcal{R} + 1)}. \quad (4.7)$$

The value reported by Darisse *et al.* (2015), which is inferred from the budgets of k and $\overline{\theta^2}/2$ measured in the same flow conditions, was $R = 0.41$ on the jet axis. Introducing the parameters listed in table 2 for Darisse *et al.* (2015), the simple model (4.7) gives $R \simeq 0.40$, which is in good agreement with the measurements.

5. Conclusions

The paper reports self-preservation analyses of the transport equations for the mean temperature and the second-order temperature structure function with a view to deriving a simple analytical expression for ϵ_θ on the axis of a slightly heated round jet. Comparison between the theoretical results and experimental data shows that complete self-preservation (i.e. self-preservation at all scales of motion) is observed on the axis of the jet. In particular, the condition for complete self-preservation, which

indicates that all the characteristic length scales must evolve linearly with x and are proportional to each other, *viz.* $\eta \propto \lambda \propto \lambda_\theta \propto R_U \propto R_\Theta \propto \hat{x}$, is very well verified by the measurements, providing confidence in the theoretical analysis. Also confirmed by the measurements, the analysis shows that both Re_λ and Pe_λ , the turbulent Reynolds and Péclet numbers, must be constant under complete self-preservation. This is of practical interest since then they can be formally used as parameters to confirm the validity of self-preservation along the jet axis. Finally, the mean temperature excess and the temperature variance must evolve like $\Theta_0 \propto \hat{x}^{-1}$ and $\overline{\theta^2} \propto \hat{x}^{-2}$ while the mixed velocity–temperature moments vary like $\overline{u\theta} \propto \hat{x}^{-2}$ and $\overline{v\theta^2} \propto \hat{x}^{-3}$.

The self-preservation analysis formally yields $\epsilon_\theta \propto \hat{x}^{-4}$, thus providing a solid analytical foundation for the derivation of the -4 th power law which characterizes the evolution along the jet axis of the mean dissipation rate of $\overline{\theta^2}/2$. The present results support and confirm the experimental observation of the -4 th power law. The analysis also leads to the following two important outcomes:

- (i) A new analytical expression for ϵ_θ on the jet axis was developed and shown to be in a good agreement with experimental data.
- (ii) New simple models are also developed for the turbulent Péclet number and the thermal-to-mechanical time scale ratio. Although the models are in reasonably good agreement with measurements, it should be kept in mind that they involve global parameters which are influenced by the boundary conditions and are therefore flow dependent.

Acknowledgements

J.L. and A.B. gratefully acknowledge the financial support of the Natural Sciences and Engineering Research Council of Canada. L.D. gratefully acknowledges the financial support of the Australian Research Council.

Appendix A. Derivation of some additional power laws

A.1. Evolution of the mean temperature excess along the jet axis

The streamwise evolution of Θ_0 is determined from the equilibrium self-preservation analysis of the mean temperature equation. Using the continuity equation, mean axisymmetry properties and the condition of high Reynolds and Péclet numbers (negligible contribution of molecular diffusion), the mean temperature equation for the slightly heated round jet can be written as

$$\frac{\partial \overline{U\Theta}}{\partial x} + \frac{1}{r} \frac{\partial r \overline{V\Theta}}{\partial r} + \frac{\partial \overline{u\theta}}{\partial x} + \frac{1}{r} \frac{\partial r \overline{v\theta}}{\partial r} \simeq 0. \tag{A 1}$$

The data of Darisse *et al.* (2014, 2015) ($Re_D = 1.4 \times 10^5$ and $Re_\lambda = 548$) show that the molecular diffusion terms are negligible – by several orders of magnitude – when compared to the dominant terms. Integration of this expression in the radial direction yields, after some manipulations,

$$\frac{\partial}{\partial x} \int_0^\infty (\overline{U\Theta} + \overline{u\theta}) r dr + (r \overline{V\Theta})|_0^\infty + (r \overline{v\theta})|_0^\infty \simeq 0. \tag{A 2}$$

Since the last two terms on the left-hand side are zero, equation (A 2) reduces to

$$\int_0^\infty (\overline{U\Theta} + \overline{u\theta}) r dr \simeq C_9, \tag{A 3}$$

where C_9 is constant. This expression represents the integral form of the energy conservation applied to the slightly heated round jet.

In a similar fashion to that reported for the velocity field by Hussein *et al.* (1994) and Ewing *et al.* (2007), we assume that the mean temperature equation admits equilibrium self-preservation solution for \bar{U} , $\bar{\Theta}$ and $\bar{u\theta}$ of the form

$$\bar{U} = U_0(x)f(r/l_\theta), \quad (\text{A } 4)$$

$$\bar{\Theta} = \Theta_0(x)g(r/l_\theta), \quad (\text{A } 5)$$

$$\bar{u\theta} = H_0(x)h(r/l_\theta), \quad (\text{A } 6)$$

where l_θ is a characteristic length scale introduced in § 2.1. For the velocity field, Thiasset *et al.* (2014) showed that the product U_0l_u is constant, l_u being the characteristic length scale. For the passive temperature field, it is shown in § 2.1 that the product U_0l_θ is constant. Thus, as the observation made for the velocity field still applied to the passive temperature field, it immediately follows that $l_\theta \propto l_u$. Consequently, the shape function $f(r/l_\theta)$ in (A 4) can also be considered as a function of r/l_u , as it is usually done for the mean streamwise velocity profile. The terms in capital letters on the right-hand sides of expressions (A 4)–(A 6) represent scales characterizing the streamwise evolution of the given quantity on the jet axis, while the lower-case functions represent the shape of the radial profile of these quantities. Introducing these forms (in which we omit to note the x and r/l_θ dependency for scale and shape functions, respectively) into (A 3) yields

$$(U_0\Theta_0l_\theta^2 + H_0l_\theta^2) \int_0^\infty (fg + h)(r/l_\theta) d(r/l_\theta) \simeq C_9. \quad (\text{A } 7)$$

The term in front of the integral involves functions of x only while the integral involves functions of r/l_θ only. The product of the two terms being constant, each of them must be constant, yielding the two following constraints:

$$U_0\Theta_0l_\theta^2 \simeq C_{10}, \quad (\text{A } 8)$$

$$H_0l_\theta^2 \simeq C_{11}, \quad (\text{A } 9)$$

where C_{10} and C_{11} are both constant. Finally, as is shown in § 2.1 that $U_0 \propto \hat{x}^{-1}$ and $l_\theta \propto \hat{x}$, the power laws for Θ_0 and H_0 immediately follow:

$$\Theta_0 \propto \hat{x}^{-1}, \quad (\text{A } 10)$$

$$H_0 \propto \hat{x}^{-2}. \quad (\text{A } 11)$$

The power law for Θ_0 is usually written as

$$\frac{\Theta_0}{\Theta_j} = B_\Theta \hat{x}^{-1}. \quad (\text{A } 12)$$

The streamwise derivative of this power law gives

$$\frac{d\Theta_0}{d\hat{x}} = -\Theta_0 \hat{x}^{-1}. \quad (\text{A } 13)$$

A.2. Longitudinal evolution of the jet half-radius

Admitting a self-preserving solution for the mean temperature excess as described by (A 5), the normalized radial profile of $\bar{\Theta}$ is written as

$$\frac{\bar{\Theta}}{\Theta_0} = g\left(\frac{r}{l_\theta}\right). \quad (\text{A } 14)$$

Let R_θ be defined as the radial location where $\bar{\Theta} = \Theta_0/2$, yielding

$$g\left(\frac{R_\theta}{l_\theta}\right) = \frac{1}{2}. \quad (\text{A } 15)$$

The shape function g being not a function of x and $g(R_\theta/l_\theta)$ being constant ($\equiv 1/2$), it immediately follows that R_θ/l_θ must be constant. Since relation (2.28) $l_\theta \propto \hat{x}$, we obtain $R_\theta \propto \hat{x}$. This confirms that R_θ , the half-radius based on the mean temperature profile, evolves linearly. The same reasoning applied to the velocity field, with R_U defining the radial location where $\bar{U} = U_0/2$, allows us to obtain $R_U \propto \hat{x}$. The usual normalized relation defining the longitudinal evolution of the half-radius based on the mean velocity profile is finally written as:

$$\frac{R_U}{D} = B_{R_U} \hat{x}, \quad (\text{A } 16)$$

where B_{R_U} is the spreading rate of the jet.

Moreover, using outer scaling R_u and Θ_0 in expression (A 13), the normalized form of the streamwise derivative of Θ_0 is written as

$$\frac{R_U}{D} \frac{1}{\Theta_0} \frac{d\Theta_0}{d\hat{x}} = -B_{R_U}. \quad (\text{A } 17)$$

REFERENCES

- ANTONIA, R. A. & MI, J. 1993 Temperature dissipation in a turbulent round jet. *J. Fluid Mech.* **250**, 531–551.
- ANTONIA, R. A., OULD-ROUIS, M., ANSELMET, F. & ZHU, Y. 1997 Analogy between predictions of Kolmogorov and Yaglom. *J. Fluid Mech.* **332**, 395–409.
- ANTONIA, R. A., SATYAPRAKASH, R. J. & HUSSAIN, A. K. M. F. 1980 Measurements of dissipation rate and some other characteristics of turbulent plane and circular jets. *Phys. Fluids* **23** (4), 695–700.
- ANTONIA, R. A., SMALLEY, R. J., ZHOU, T., ANSELMET, F. & DANAILA, L. 2004 Similarity solution of temperature structure functions in decaying homogeneous isotropic turbulence. *Phys. Rev. E* **69**, 016305.
- ANTONIA, R. A. & VAN ATTA, C. W. 1978 Structure functions of temperature fluctuations in turbulent shear flows. *J. Fluid Mech.* **84**, 561–580.
- BURATTINI, P., ANTONIA, R. A. & DANAILA, L. 2005a Scale-by-scale energy budget on the axis of a turbulent round jet. *J. Turbul.* **6**, 1–11.
- BURATTINI, P., ANTONIA, R. A. & DANAILA, L. 2005b Similarity in the far field of a turbulent round jet. *Phys. Fluids* **17**, 1–14.
- CHEVRAY, R. & TUTU, N. K. 1978 Intermittency and preferential transport of heat in a round jet. *J. Fluid Mech.* **88** (01), 133–160.

- DANAÏLA, L., ANSELMET, F., ZHOU, T. & ANTONIA, R. A. 1999 A generalization of Yaglom's equation which accounts for the large-scale forcing in heated decaying turbulence. *J. Fluid Mech.* **391**, 359–372.
- DANAÏLA, L., KRAWCZYNSKI, J. F., THIESSET, F. & RENO, B. 2012 Yaglom-like equation in axisymmetric anisotropic turbulence. *Physica D* **241** (3), 216–223.
- DARISSE, A., LEMAY, J. & BENAÏSSA, A. 2013a Investigation of passive scalar mixing in a turbulent free jet using simultaneous LDV and cold wire measurements. *Intl J. Heat Fluid Flow* **44**, 284–292.
- DARISSE, A., LEMAY, J. & BENAÏSSA, A. 2013b LDV measurements of well converged third order moments in the far field of a free turbulent round jet. *Exp. Therm. Fluid Sci.* **44**, 825–833.
- DARISSE, A., LEMAY, J. & BENAÏSSA, A. 2014 Extensive study of temperature dissipation measurements on the centerline of a turbulent round jet based on the $\overline{\theta^2}/2$ budget. *Exp. Fluids* **55** (1), 1–15.
- DARISSE, A., LEMAY, J. & BENAÏSSA, A. 2015 Budgets of turbulent kinetic energy, Reynolds stresses, variance of temperature fluctuations and turbulent heat fluxes in a round jet. *J. Fluid Mech.* **774**, 95–142.
- DEKEYSER, I. & LAUNDER, B. E. 1983 A comparison of triple-moment temperature-velocity correlations in the asymmetric heated jet with alternative closure models. In *Turbulent Shear Flows 4* (ed. L. J. S. Bradbury, F. Durst, B. E. Launder, F. W. Schmidt & J. H. Whitelaw), pp. 102–117. Springer.
- DJENIDI, L., ANTONIA, R. A., LEFEUVRE, N. & LEMAY, J. 2016 Complete self-preservation on the axis of a turbulent round jet. *J. Fluid Mech.* **790**, 57–70.
- EWING, D., FROHNAPFEL, B., GEORGE, W. K., PEDERSEN, J. M. & WESTERWEEL, J. 2007 Two-point similarity in the round jet. *J. Fluid Mech.* **577**, 309–330.
- FRIEHE, C. A., VAN ATTA, C. W. & GIBSON, C. H. 1971 Jet turbulence: dissipation rate measurements and correlations. *Turbulent Shear Flows, AGARD CP-93*, pp. 18.1–18.7.
- GIBSON, M. M. & LAUNDER, B. E. 1976 On the calculation of horizontal, turbulent, free shear flows under gravitational influence. *ASME J. Heat Transfer* **98** (1), 81–87.
- HANJALIĆ, K. & LAUNDER, B. 2011 *Modelling Turbulence in Engineering and the Environment: Second-Moments Routes to Closure*. Cambridge University Press.
- HILL, R. J. 1997 Applicability of Kolmogorov's and Monin's equations of turbulence. *J. Fluid Mech.* **353**, 67–81.
- HILL, R. J. 2001 Equations relating structure functions of all orders. *J. Fluid Mech.* **434**, 379–388.
- HUSSEIN, H. J., CAPP, S. P. & GEORGE, W. K. 1994 Velocity measurements in a high-Reynolds-number, momentum-conserving, axisymmetric, turbulent jet. *J. Fluid Mech.* **258**, 31–75.
- LEMAY, J., BENAÏSSA, A. & ANTONIA, R. A. 2003 Correction of cold-wire response for mean temperature dissipation rate measurements. *Exp. Therm. Fluid Sci.* **27** (2), 133–143; 6th International Thermal Anemometry Symposium.
- LEMAY, J. & BENAÏSSA, A. 2001 Improvement of cold-wire response for measurement of temperature dissipation. *Exp. Fluids* **31**, 347–356.
- LEMOINE, F., ANTOINE, Y., WOLFF, M. & LÉBOUCHE, M. 1999 Simultaneous temperature and 2D velocity measurements in a turbulent heated jet using combined laser-induced fluorescence and LDA. *Exp. Fluids* **26**, 315–323.
- MI, J., XU, M. & ZHOU, T. 2013 Reynolds number influence on statistical behaviors of turbulence in a circular free jet. *Phys. Fluids* **25**, 075101.
- PANCHAPAKESAN, N. R. & LUMLEY, J. L. 1993a Turbulence measurements in axisymmetric jets of air and helium. Part 1. Air jet. *J. Fluid Mech.* **246**, 197–223.
- PANCHAPAKESAN, N. R. & LUMLEY, J. L. 1993b Turbulence measurements in axisymmetric jets of air and helium. Part 2. Helium jet. *J. Fluid Mech.* **246**, 225–247.
- PIETRI, L., AMIELH, M. & ANSELMET, F. 2000 Simultaneous measurements of temperature and velocity fluctuations in a slightly heated jet combining a cold wire and Laser Doppler Anemometry. *Intl J. Heat Fluid Flow* **21** (1), 22–36.
- POPE, S. B. 2000 *Turbulent Flows*. Cambridge University Press.

- RUFFIN, E., SCHIESTEL, R., ANSELMET, F., AMIELH, M. & FULACHIER, L. 1994 Investigation of characteristic scales in variable density turbulent jets using a second-order model. *Phys. Fluids* **6** (8), 2785–2799.
- SHIVAMOGGI, B. K. & ANTONIA, R. A. 2000 Isotropic and axisymmetric turbulence of passive scalars. *Fluid Dyn. Res.* **26**, 95–104.
- TENNEKES, H. & LUMLEY, J. L. 1972 *A First Course in Turbulence*. MIT Press.
- THIESSET, F., ANTONIA, R. A. & DJENIDI, L. 2014 Consequences of self-preservation on the axis of a turbulent round jet. *J. Fluid Mech.* **748**, R2.
- YAGLOM, A. M. 1949 On the local structure of the temperature field in a turbulent flow. *Dokl. Akad. Nauk SSSR* **69**, 743–746.